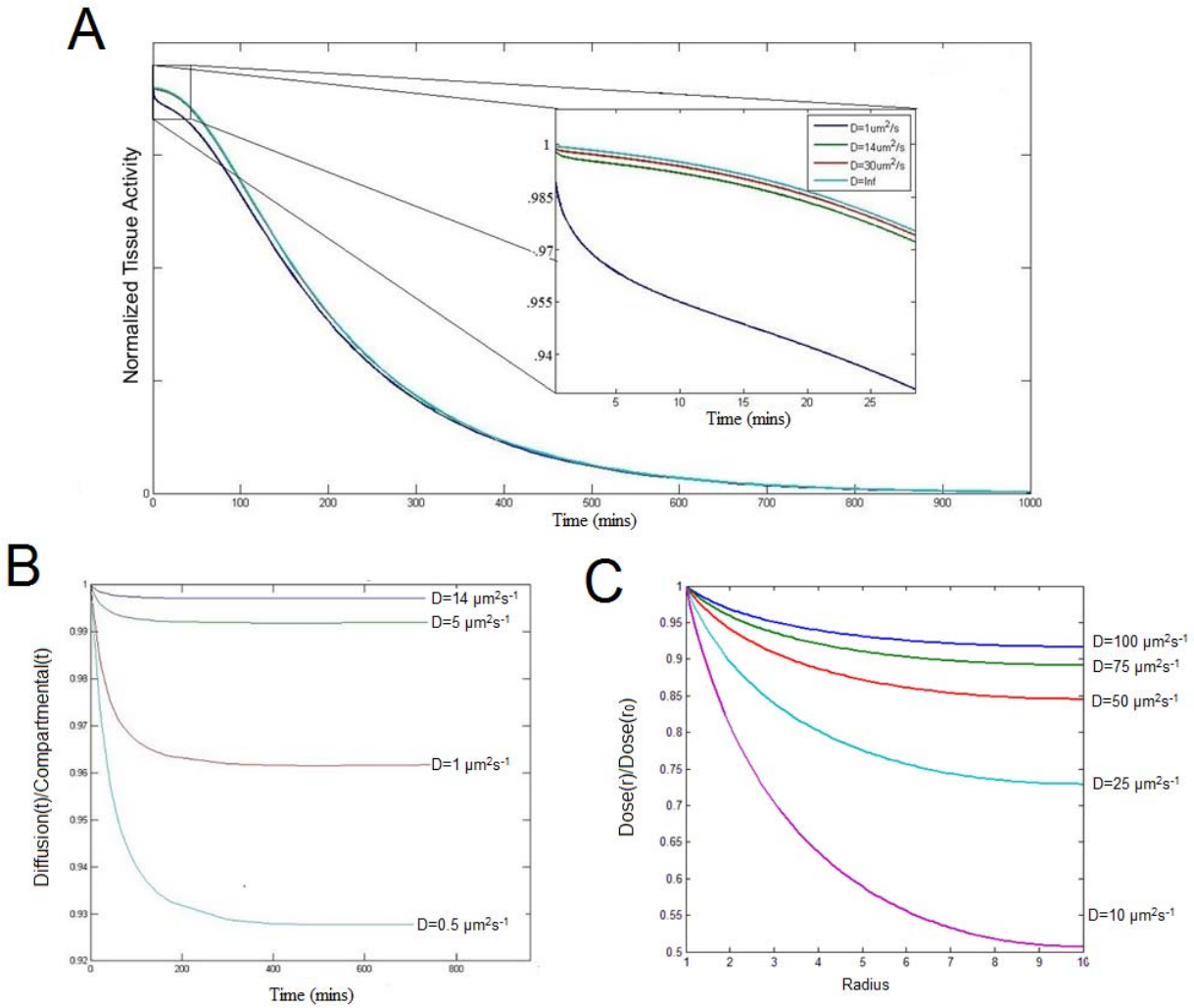
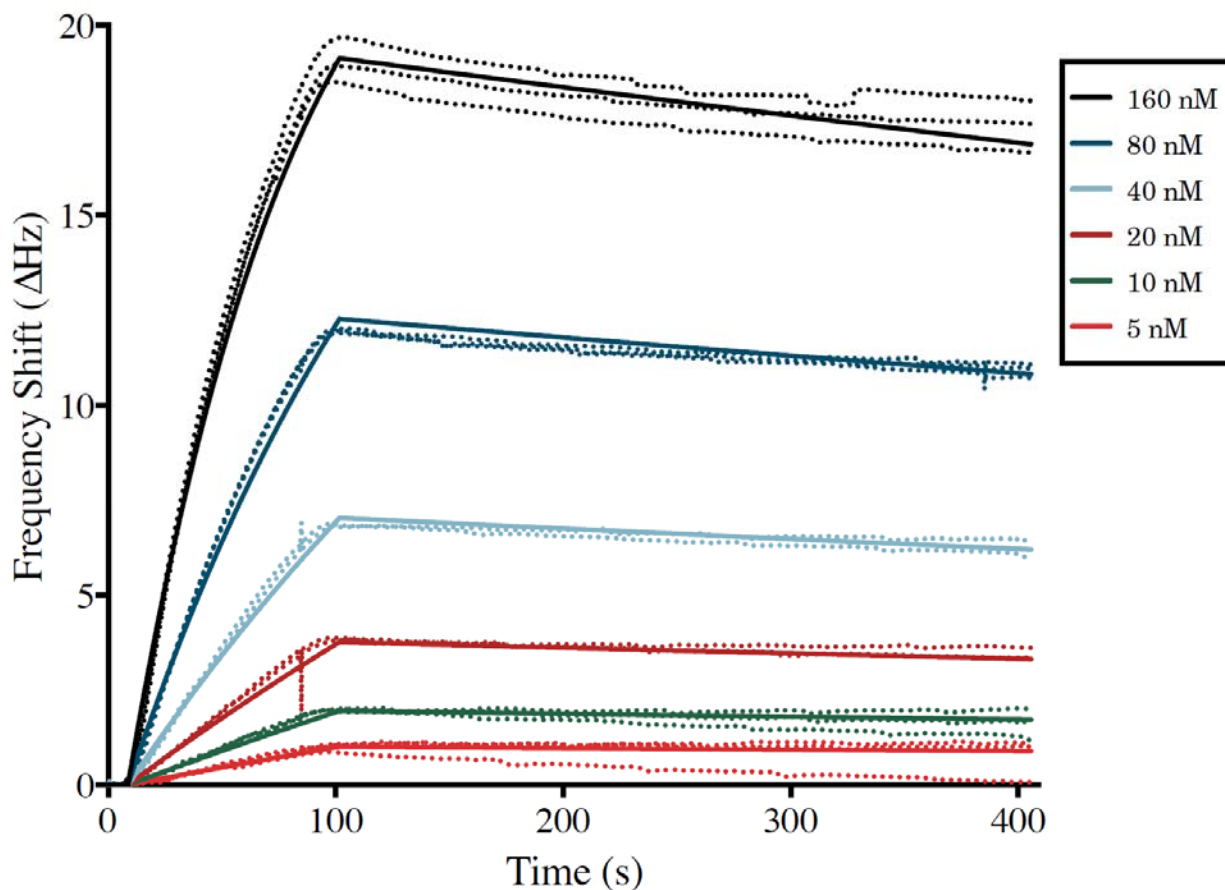


Supplemental Figures

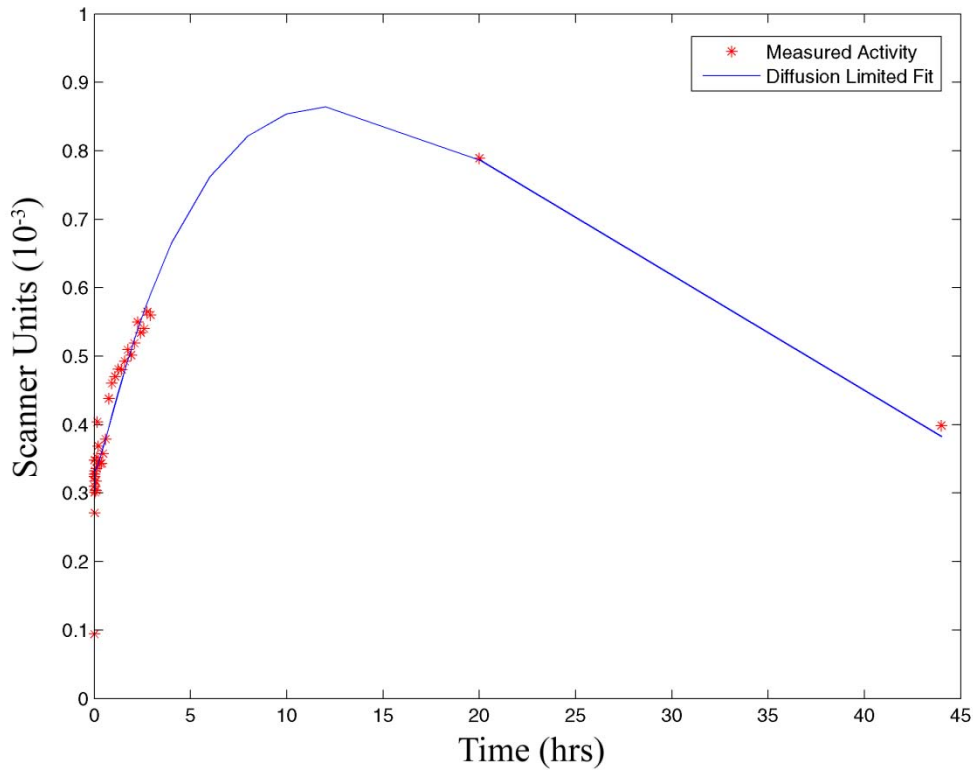


SUPPLEMENTAL FIGURE 1. Effects of diffusion on TACs and dose-at-depth in linear binding models. (A) Simulated TAC in response to unit impulse at different rates of diffusion. Curves are normalized by the maximum simulated value from the infinite diffusion curve. (B) Ratio of simulated TACs at different diffusion rates to an infinite diffusion model. Even at biologically unreasonable rates ($D=1 \mu\text{m}^2/\text{s}^{-1}$), differences are less than 5%. (C) Total dose at depth relative to dose at capillary wall as a function of diffusion rates.

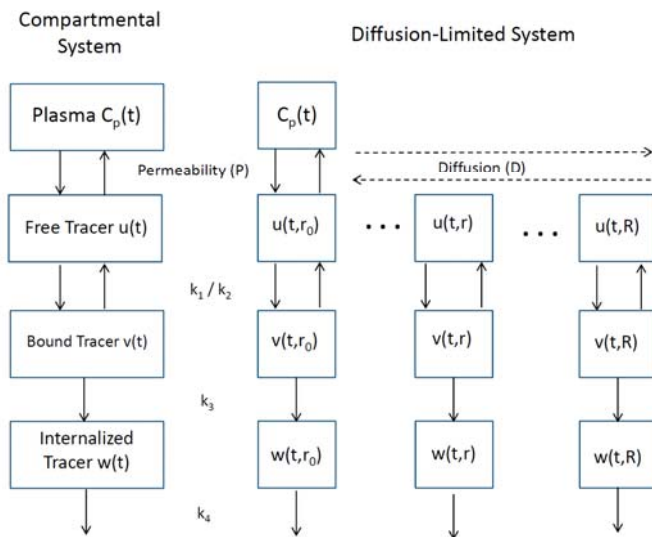


| | k_{on} ($\text{M}^{-1}\text{s}^{-1}$) | k_{off} (s^{-1}) | B_{Max} | K_{D} (nM) |
|--------------|--|--------------------------------------|------------------|---------------------|
| A11 Minibody | 1.21×10^5 | 4.95×10^{-4} | 25.27 | 4.14 |

SUPPLEMENTAL FIGURE 2. Affinity Measurements of A11 minibody, immobilized PSCA antigen as measured by quartz crystal microbalance. Bold line is the mass transport limited binding model fit from $n = 3$ measurements at each concentration (160-5 nM), shown as dotted lines.



SUPPLEMENTAL FIGURE 3. Fitting of TAC measured from 22Rv1xPSCA tumor in second mouse using diffusion limited model with Bayesian Priors.



SUPPLEMENTAL FIGURE 4. Illustration of difference between a standard compartmental model and the diffusion-limited case.

Derivation of Kinetic Models

Motivation

In a standard compartmental model, transport of a tracer between well-mixed compartment is modeled as a series of ordinary differential equations (ODEs). However, in the case of heterogeneously localized tracers, these compartments are no longer well-mixed, and the spatial concentration of the tracer must be modeling within each compartment. This effectively leads to a set of linked compartmental models at each location in tissue (Supplemental Figure 4). In the case of tracer kinetics within tumors, it is natural to model this heterogeneous localization as diffusion of tracer away from the capillary wall into tissue in a radially symmetric fashion. Therefore, in the case of diffusion-limited tracers, we model tissue as a collection of identical cylinders, each with a central capillary enervating the tissue within that cylinder. The problem can be further simplified, by only examining 2-D slices of tissue (orthogonal to the capillary), as there will be no net diffusion between such slices. By converting equations to a radially symmetric geometry, we can thus reduce the system to a single spatial dimension.

1 - General Model Form - Linear Binding Kinetics

We examine radially symmetric diffusion of our compound. Let $u(r, t)$ = unbound compound, $v(r, t)$ = bound compound, and $w(r, t)$ = compound internalized into the cell. We then assume the following about our system:

- (i) Plasma concentration of the compound is $C_p(t)$.
- (ii) Compound moves reversibly into/out of the tissue at a rate defined by the capillary permeability, P .
- (iii) The compound binds/unbinds to surface receptors at rates k_1, k_2 , respectively.
- (iv) The bound compound is reversibly endo/exocytosed at rates k_3, k_4 .
- (v) The internalized compound is irreversibly metabolized out of the system at rate k_5 .
- (vi) Lastly, the compound diffuses linearly through tissue at rate D .

In the case of infinitely fast diffusion (i.e. classical compartmental model), we can describe the system with the following set of ODEs.

$$\begin{aligned}\frac{d}{dt}u(t) &= PCp(t) - (k_1 + P)u(t) + k_2v(t) \\ \frac{d}{dt}v(t) &= k_1u(r, t) + k_4w(t) - (k_2 + k_3)v(t) \\ \frac{d}{dt}w(t) &= k_3v(r, t) - (k_4 + k_5)w(t)\end{aligned}\tag{1}$$

In the case of finite diffusion rates, the following set of PDEs describe the system.

$$\begin{aligned}\frac{\delta}{\delta t}u(r, t) &= D\left[\frac{\delta^2}{\delta r^2}u(r, t) + \frac{1}{r}\frac{\delta}{\delta r}u(r, t)\right] - k_1u(r, t) + k_2v(r, t) \\ \frac{\delta}{\delta t}v(r, t) &= k_1u(r, t) + k_4w(r, t) - (k_2 + k_3)v(r, t) \\ \frac{\delta}{\delta t}w(r, t) &= k_3v(r, t) - (k_4 + k_5)w(r, t)\end{aligned}\tag{2}$$

For the PDE system, two Neumann boundary conditions are required:

$$\begin{aligned} -D \frac{\delta}{\delta r} u(r, t) \Big|_{r=r_o} &= PC_p(t) - Pu(r_o, t) \\ \frac{\delta}{\delta r} u(R, t) &= 0 \end{aligned} \quad (3)$$

The first corrects for the rate of influx/efflux of tracer from the capillaries which are centered at $r = 0$ and have radius r_o . The second corrects for diffusion of tracer out of the radius $r = R$ disc. Mathematically this actually manifests as a "reflective boundary" but we can think of it as correcting for influx from adjacent discs. This is not exactly correct as not all points on the discs are radius $r = R$ from two capillaries. However, this should still give the analytically correct result as we integrate over the disc because diffusion and compartmental transport are constant over radii, so in this formulation we are doing the same thing as integrating over all $r > r_o$ with no boundary condition on the outer radius.

2 - Solving the General Form

No analytical solution to the PDEs described above in equation (2) exist in the time domain. However, by applying a Laplace transform, an analytical solution is yielded.

Applying the Laplace transform yields the following differential equations.

$$\begin{aligned} s\hat{u}(r, s) &= D \left[\frac{\delta^2}{\delta r^2} \hat{u}(r, s) + \frac{1}{r} \frac{\delta}{\delta r} \hat{u}(r, s) \right] - k_1 \hat{u}(r, s) + k_2 \hat{v}(r, s) \\ s\hat{v}(r, s) &= k_1 \hat{u}(r, s) + k_4 \hat{w}(r, s) - (k_2 + k_3) \hat{v}(r, s) \\ s\hat{w}(r, s) &= k_3 \hat{v}(r, s) - (k_4 + k_5) \hat{w}(r, s) \end{aligned} \quad (4)$$

We begin our solution by simplifying the algebraic relation between $\hat{u}(r, s)$, $\hat{v}(r, s)$, and $\hat{w}(r, s)$

$$\begin{aligned} \hat{w}(r, s) &= \frac{k_3}{s + k_4 + k_5} \hat{v}(r, s) = C_w \hat{v}(r, s) \\ \rightarrow s\hat{v}(r, s) &= k_1 \hat{u}(r, s) + k_4 C_w \hat{v}(r, s) - (k_2 + k_3) \hat{v}(r, s) \\ &\rightarrow \hat{v}(r, s) [s + k_2 + k_3 - k_4 C_w] = k_1 \hat{u}(r, s) \\ \rightarrow \hat{v}(r, s) &= \frac{k_1}{s + k_2 + k_3 - k_4 C_w} \hat{u}(r, s) = C_v \hat{u}(r, s) \\ D \left[\frac{\delta^2}{\delta r^2} \hat{u}(r, s) + \frac{1}{r} \frac{\delta}{\delta r} \hat{u}(r, s) \right] &- (s + k_1 - k_2 C_v) \hat{u}(r, s) = 0 \\ \rightarrow r^2 \frac{\delta^2}{\delta r^2} \hat{u}(r, s) + r \frac{\delta}{\delta r} \hat{u}(r, s) &- r^2 C_s^2 \hat{u}(r, s) = 0 \\ \text{Where } C_s^2 &= \frac{1}{D} (s + k_1 - k_2 C_v) \end{aligned} \quad (5)$$

The resulting simplified equation can be solved more easily after applying a change a variables: $\rho = rC_s$

$$\begin{aligned}
 & \rho^2 \frac{1}{C_s^2} \frac{\delta^2}{\delta r^2} \hat{u}(\rho, s) + \rho \frac{1}{C_s} \frac{\delta}{\delta r} \hat{u}(\rho, s) - \rho^2 \hat{u}(\rho, s) = 0 \\
 \rightarrow & \rho^2 \left(\frac{dr}{d\rho}\right)^2 \frac{\delta^2}{\delta r^2} \hat{u}(\rho, s) + \rho \frac{dr}{d\rho} \frac{\delta}{\delta r} \hat{u}(\rho, s) - \rho^2 \hat{u}(\rho, s) = 0 \\
 \rightarrow & \rho^2 \frac{\delta^2}{\delta \rho^2} \hat{u}(\rho, s) + \rho \frac{\delta}{\delta \rho} \hat{u}(\rho, s) - \rho^2 \hat{u}(\rho, s) = 0 \\
 \rightarrow & \boxed{\hat{u}(r, s) = \alpha(s)I_0(rC_s) + \beta(s)K_0(rC_s)} \tag{6}
 \end{aligned}$$

As shown in equations (6), $\hat{u}(\rho, s)$ is a sum of modified Bessel functions of order zero :

$\hat{u}(\rho, s) = \alpha(s)I_0(\rho) + \beta(s)K_0(\rho)$, where $\alpha(s), \beta(s)$ are constant in r and will be defined by our boundary conditions.

3 - Solving the Boundary Conditions

At the $r = R$ boundary, the Laplace transform yields:

$$\begin{aligned}
 \frac{\delta}{\delta r} u(R, t) = 0 \rightarrow & \alpha(s)C_s I_1(RC_s) - \beta(s)C_s K_1(RC_s) = 0 \\
 \rightarrow & \boxed{\beta(s) = \alpha(s) \frac{I_1(RC_s)}{K_1(RC_s)} = \alpha(s)I_K} \\
 \text{Where } & \boxed{I_K = \frac{I_1(RC_s)}{K_1(RC_s)}} \tag{7}
 \end{aligned}$$

Taking the Laplace transform of the $r = r_o$ boundary condition yields the following:

$$\begin{aligned}
 -D \frac{\delta}{\delta r} \hat{u}(r, t)|_{r=r_o} &= P\hat{C}_p(t) - P\hat{u}(r_o, s) \\
 \boxed{\frac{d}{dr} I_0(rC_s) = C_s I_1(rC_s) \quad \frac{d}{dr} K_0(rC_s) = -C_s K_1(rC_s)} \\
 \rightarrow D\alpha(s)C_s [I_K K_1(r_o C_s) - I_1(r_o C_s)] &= P\hat{C}_p(s) - P\alpha(s)[I_0(r_o C_s) + K_0(r_o C_s)] \\
 \boxed{\alpha(s) = \frac{P\hat{C}_p(s)}{DC_s [I_K K_1(r_o C_s) - I_1(r_o C_s)] + P[I_0(r_o C_s) + I_K K_0(r_o C_s)]}} \tag{8}
 \end{aligned}$$

4 - Infinite Diffusion Limit

We want to make sure this correctly model behaviors in the infinitely fast diffusion limit (the standard compartmental model). In Laplace space, the solution to the comparable compartmental model is, trivially, as follows:

$$\begin{aligned}\hat{w}(s) &= C_w v(s) \\ \hat{v}(s) &= C_v u(s) \\ \hat{u}(s) &= \frac{\tilde{P} \hat{C}_p(s)}{s + \tilde{P} + k_1 - C_v k_2} \\ \tilde{P} &= (2\pi r_o) \frac{P}{\pi(R^2 - r_o^2)}\end{aligned}\tag{9}$$

With C_w, C_v defined as above. Here \tilde{P} is modified to correct for the differences between this "compartmental" model and the radially symmetric "Diffusion Model". The $\frac{1}{\pi(R^2 - r_o^2)}$ term is to correct for the fact that with infinite diffusion, transport in/out of tissue to/from capillaries is placed evenly across all radii, so influx and efflux are reduced by a factor proportional to the area enervated by the capillary in question. The $(2\pi r_o)$ is to correct for the fact that in the "Diffusion" model, P is a measure of flux across an infinitesimal point on the capillary wall, but in the "Compartmental" model it refers to the net-flux across the entire circumference of the capillary.

In the $D \rightarrow \infty, C_s \rightarrow 0$ limit, the solution from part 3 (Eqs. 6-8) should simplify to the above solution (Eqs. 9).

In the large D , small C_s limit, we have the following asymptotic approximations for the modified Bessel functions:

$$\begin{aligned}\lim_{z \rightarrow 0} I_0(z) &\sim 1 \\ \lim_{z \rightarrow 0} I_1(z) &\sim \frac{z}{2} \\ \lim_{z \rightarrow 0} K_0(z) &\sim -\ln(z) \\ \lim_{z \rightarrow 0} K_1(z) &\sim \frac{1}{z}\end{aligned}$$

$$\rightarrow \lim_{C_s \rightarrow 0} I_K = \lim_{C_s \rightarrow 0} \frac{I_1(RC_s)}{K_1(RC_s)} = \frac{RC_s}{2(RC_s)^{-1}} = \frac{(RC_s)^2}{2}$$

We can then use this information to get an asymptotic estimate of $\alpha(s)$ in the large D limit:

$$\begin{aligned} \lim_{C_s \rightarrow 0} \alpha(s) &= \lim_{C_s \rightarrow 0} \frac{P\hat{C}_p(s)}{DC_s \left[\frac{(RC_s)^2}{2} \frac{1}{r_0 C_s} - \frac{r_0 C_s}{2} \right] + P \left[1 - \frac{(RC_s)^2}{2} \ln(r_0 C_s) \right]} = \frac{P\hat{C}_p(s)}{\frac{DC_s^2}{2r_0} [R^2 - r_0^2] + P} \\ &\rightarrow \lim_{C_s \rightarrow 0} \alpha(s) = \frac{\frac{P}{[R^2 - r_0^2]} \hat{C}_p(s)}{\frac{1}{2r_0} (s + k_1 - k_2 C_v) + \frac{P}{[R^2 - r_0^2]}} = \frac{\tilde{P}\hat{C}_p(s)}{s + \tilde{P} + k_1 - k_2 C_v} \\ \rightarrow \lim_{D \rightarrow \infty} \hat{u}(r, s) &= \lim_{D \rightarrow \infty} \alpha(s) [I_o(rC_s) + I_K K_o(rC_s)] = \lim_{D \rightarrow \infty} \alpha(s) \left[1 - \frac{(RC_s)^2}{2} \ln(rC_s) \right] = \lim_{D \rightarrow \infty} \alpha(s) \\ \lim_{D \rightarrow \infty} \alpha(s) &= \lim_{C_s \rightarrow \infty} \alpha(s) = \boxed{\frac{\tilde{P}\hat{C}_p(s)}{(s + \tilde{P} + k_1 - k_2 C_v)}} \end{aligned}$$

Thus, the model specified by Eqs. 2-3 converges to the standard compartmental model (Eqs. 1) in the infinite diffusion limit, as specified by Eqs. 9.

5 - General Model Form - Nonlinear Binding Kinetics

As mentioned in the main body, linear binding kinetics will not always be sufficient for describing the system *in vivo*. To describe such a system, we build equations with assumptions similar to those specified in section 1. However, in addition to modeling the concentrations of tracer in extracellular space ($u(r, t)$), bound to the surface ($v(r, t)$), and internalized within the cell ($w(r, t)$), we now also track the concentration of open binding sites on the cell surface ($x(r, t)$). In this system we make the following assumptions, which result in Eqs. 10-11.

- (i) Plasma concentration of the compound is $C_p(t)$.
- (ii) Compound moves reversibly into/out of the tissue at a rate defined by the capillary permeability, P .
- (iii) The compound binds/unbinds nonlinearly to surface receptors at rates k_1, k_2 , respectively.
- (iv) Surface receptors have a steady state concentration of $dens_o$.
- (v) The concentration of open receptors returns asymptotically to steady state at rate k_{regen} .
- (vi) The bound compound/receptor complex is reversibly endo/exocytosed at rates k_3, k_4 .
- (vi) The internalized compound is irreversibly metabolized out of the system at rate k_5 .
- (vii) Lastly, the compound diffuses linearly through tissue at rate D .

In the case of infinitely fast diffusion (i.e. classical compartmental model), we can describe the system with the following set of non-linear ODEs.

$$\begin{aligned} \frac{d}{dt} u(t) &= PCp(t) - (k_1 x(t) + P)u(t) + k_2 v(t) \\ \frac{d}{dt} v(t) &= k_1 u(t)x(t) + k_4 w(t) - (k_2 + k_3)v(t) \\ \frac{d}{dt} x(t) &= -k_1 u(t)x(t) + k_2 v(t) + k_{regen}(dens_o - x(t)) \\ \frac{d}{dt} w(t) &= k_3 v(t) - (k_4 + k_5)w(t) \end{aligned} \tag{10}$$

In the case of finite diffusion rates, the following set of non-linear PDEs describe the system.

$$\begin{aligned}
 \frac{\delta}{\delta t} u(r, t) &= D \left[\frac{\delta^2}{\delta r^2} u(r, t) + \frac{1}{r} \frac{\delta}{\delta r} u(r, t) \right] - k_1 u(r, t) x(r, t) + k_2 v(r, t) \\
 \frac{\delta}{\delta t} v(r, t) &= k_1 u(r, t) x(r, t) - (k_2 + k_3) v(r, t) \\
 \frac{\delta}{\delta t} x(r, t) &= -k_1 u(r, t) x(r, t) + k_{regen} (dens_o - x(r, t)) + k_2 v(r, t) \\
 \frac{\delta}{\delta t} w(r, t) &= k_3 v(r, t) - (k_4 + k_5) w(r, t)
 \end{aligned}
 \tag{11}$$

The model described in Eqs. 11 is subject to the same Neumann boundary constraints described in Eq. 3 for the linear binding-kinetic model. Unlike the linear-binding scenario, the inclusion of nonlinear binding kinetics precludes analytical solutions in both the time and Laplace domain. Therefore, all solutions to these equations must be computed numerically.

6 - Computing Numerical Solutions

As analytical solutions to the linear binding model are readily available in the Laplace domain, solutions to these equations were computed using a numerical Laplace inversion. The solutions described in section 3 were inverted using De Hoog's numerical Laplace inversion (1), as implemented for MATLAB by Hollenbeck (2). Time activity curves were simulated by numerically inverting solutions to the Eqs. 2, and integrating the activities across radii. Solutions to Eqs. 11 were computed by applying the method of lines to discretize the spatial dimension, and numerically solving the resulting system with Runge-Kutta methods as implemented in MATLAB.

References

1. De Hoog FR, Knight J, Stokes A. An improved method for numerical inversion of Laplace transforms. *SIAM Journal on Scientific and Statistical Computing*. 1982;3(3):357-366.
2. Hollenbeck, K. J. (1998) INVLAP.M: A matlab function for numerical inversion of Laplace transforms by the de Hoog algorithm, <http://www.isva.dtu.dk/staff/karl/invlap.htm>